J6.8 SURFACE LAYER COUNTER-GRADIENT MOTION IN AND AROUND AN URBAN AREA

Cheryl L. Klipp*, Y. Wang, S. S. Chang, C. C. Williamson, G. D. Huynh, D. M. Garvey
U.S. Army Research Laboratory, Adelphi, MD 20783

ABSTRACT

Quadrant analysis of turbulent momentum flux, $\overline{u'w'}$, typically focuses on updrafts of slow fluid (quadrant 2, ejections) and downdrafts of fast fluid (quadrant 4, sweeps). The counter-gradient contributions of quadrant 1 (upward motion of fast fluid) and quadrant 3 (downward motion of slow fluid) to $\overline{u'w'}$ are typically small. Analysis of 3D sonic anemometer data from JU2003 found persistent quadrant 1 and quadrant 3 events corresponding to eddy sizes on the order of 100m. Although these events had a significant effect on less than 1% of the momentum flux calculations for the entire month of the field campaign, they may be relevant to transport and dispersion. Also discussed are the conditions prevalent during these events and some possible mechanisms which give rise to significant quadrant 1 and quadrant 3 motions.

1. INTRODUCTION

In the atmospheric surface layer, wind speeds increase with height. In general this results in updrafts transporting slower surface fluid up and downdrafts transporting faster fluid toward the surface. The resulting momentum transport is toward the surface. The magnitude of this turbulent momentum transport is an important component of theories and models and as a result is an important variable to measure in surface layer turbulence analysis.

This paper focuses on several anomalous measurements where momentum is seemingly transported upward and compares them to more standard conditions.

2. DATA

The Army Research Laboratory (ARL) deployed an array of sonic anemometers mounted on five towers in Oklahoma City, Oklahoma, during the Joint Urban 2003 field campaign, a cooperative undertaking to study turbulent transport and dispersion in the atmospheric boundary layer within an urban environment. The towers were located in a variety of locations to sample both industrial (urban) and semi-rural (suburban) conditions. Data from one of these towers will be used for this analysis: a suburban location with relatively few local obstructions.

All towers had sonic anemometers at 10 meter and 5 meter elevations measuring the three components of the wind vector at a rate of 10 samples per second. The 10m sonics were mounted above the tower, so little influence is expected from the tower for these instruments. The 5m instruments were mounted due south of the tower.

The counter gradient motions studied in this report occurred at all five of the towers at about the same times and with approximately equal frequency. No correlation has been found to indicate the movement across the area of a triggering event. Since the counter-gradient motions occur evenly across the urban and suburban area, the data from the tower with the fewest local obstructions is focused on to avoid the complication of local obstructions.

3. QUADRANT ANALYSIS

3.1. Typical case

Turbulent momentum transport is measured as $\overline{u'w'}$, where u and w are the streamwise and vertical components of the wind vector, the primes denote deviation from the means and the overbar indicates the average of the product of the deviations. For this study the deviations are computed from the 10 minute means. Quadrant analysis (Raupach 1981) studies the relative contributions to the momentum flux of updrafts of slower fluid (ejections, $u' < 0$ and $w' > 0$, quadrant 2) to downdrafts of faster fluid (sweeps, $u' > 0$, $w' < 0$, quadrant 4). The contributions from the counter gradient motions of updrafts of faster fluid (outward interactions, $u' > 0$, $w' > 0$,

* *Corresponding author address*: Cheryl Klipp, U.S. Army Research Laboratory, AMSRD-ARL-CI-EM, Adelphi, MD 02783-1197; email: cklipp@arl.army.mil.

quadrant 1) and downdrafts of slower fluid (inward interactions, $u' < 0$, $w' < 0$, quadrant 3) are usually negligible, (table 1, figure 1).

Table 1 The contribution from each quadrant to the total mean momentum flux for 2105-2115 UTC, 7 July 2003 and the percentage of points in each quadrant. For this 10-minute segment $\overline{u'w'} = -0.605$, R = –0.42.

	u'w' (m^2s^{-2})	Time fraction
1	+0.089	16%
2	-0.414	33%
3	+0.091	19%
4	-0.371	32%

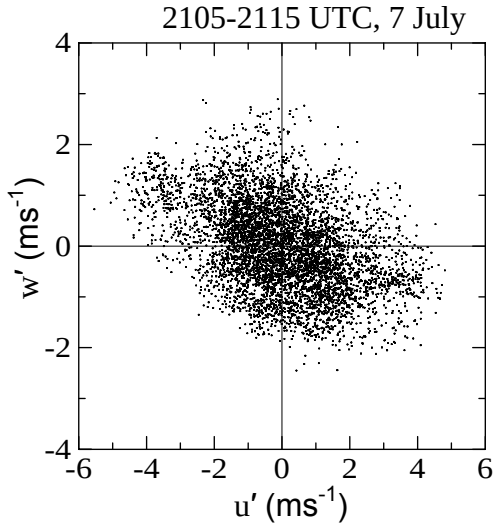

Figure 1 Quadrant plot of a typical 10-minute segment of 10 Hz data.

In addition to the $\overline{u'w'}$ contributions from each quadrant it is also informative to note the percentage of points that are in each quadrant. This is called the time fraction. The Reynolds stress correlation, $R = \overline{u'w'}/\sigma_u\sigma_w$, is another statistic of interest for this study but is not typical of quadrant analysis.

As is typical of most quadrant analyses, not only are the most significant contributions to the momentum flux due to quadrants 2 and 4, but there are more data points in those quadrants (table1). In addition, the scatter of points is not circular, thus the correlation is fairly high.

3.2. Counter-gradient case

For a very small number of 10-minute segments, the momentum flux is calculated to be upwards. In these cases the contributions from quadrants 1 and 3 become larger than the contributions from quadrants 2 and 4. In addition, the percentage of time spent in each quadrant approaches 25% (Table 2). The clustering of the points closer to the origin in Figure 2 is a result of the overall lower TKE at this time compared to the typical case in Figure 1.

Table 2 The contribution from each quadrant to the total mean momentum flux for 1710-1720 UTC, 2 July 2003 and the percentage of points in each quadrant. For this 10-minute segment $\overline{u'w'} = +0.082$, R = +0.11.

	u'w' (m^2s^{-2})	Time fraction
1	+0.190	23%
2	-0.121	24%
3	+0.102	29%
4	-0.089	24%

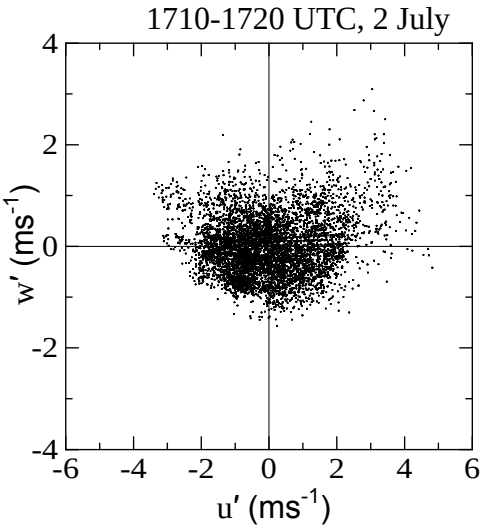

Figure 2 Quadrant plot of an atypical 10-minute segment of 10 Hz data.

4. DISCUSSION

4.1. Large Scale Structure

Although quadrant analysis is meant to examine the properties of the large scale coherent motion

within a turbulent flow, large scale structures are not evident in the quadrant plots (Robinson 1991). The time series plots do show coherent structure (figure 3).

The largest scale events in Figure 3 are on the order of 30 seconds in duration. With the mean wind speed of 4.0 ms^{-1}, this translates to a horizontal scale on the order of 120 meters. The boundary layer depth at this time was about 1100m.

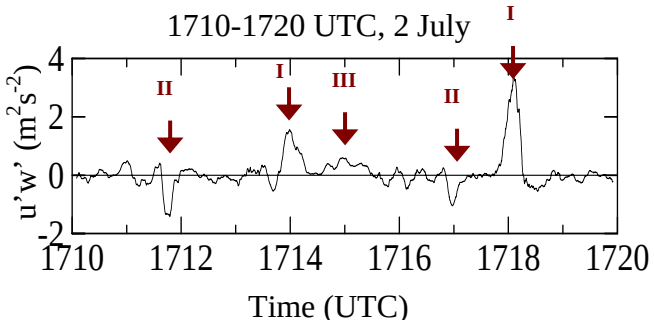

Figure 3 Time series of an atypical 10-minute segment of 10 Hz data. A 10 second running mean filter applied to remove effects of smaller scales of turbulence. The quadrants associated with some of the larger are labeled.

4.2. Stationarity

The quadrant analysis, as are the flux calculations, is very dependent on instrument tilt. Due to the complex urban environment at most of the tower locations, the planar tilt method of tilt correction is not appropriate (Wilczak *et al*. 2001), so the older method of setting $\overline{V} = \overline{W} = 0$ has been used. Each data segment has been subjected to wind direction variance criteria to ensure that this method of instrument tilt correction is appropriate. Since the location used in this analysis has very few local obstructions, the analysis was repeated using planar tilt corrected data. The same results were found using a planar tilt corrected version of the data.

4.3. Synoptic Scale Occurrence

As can be seen in figure 4, the anomalous positive daytime values of $\overline{u'w'}$ (1400-2295 UTC) are the extension of a pattern of momentum flux values throughout the month of the field campaign. The days of relatively small $\overline{u'w'}$ values coincide with the passage of cold fronts the day or evening before. Figure 5 shows the same plot for night time (0300-1059 UTC). Although the synoptic scale pattern is the same, there are no significant upward momentum fluxes at night.

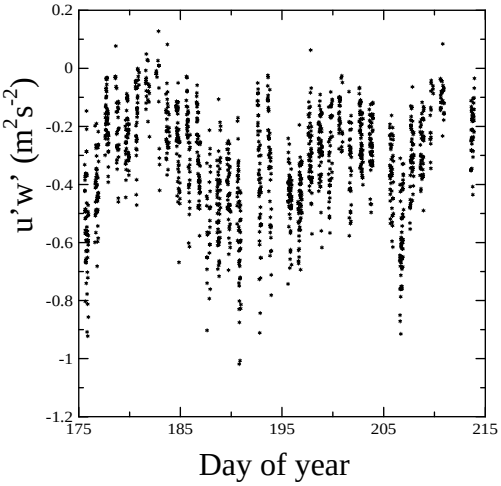

Figure 4 Calculated values of daytime $\overline{u'w'}$ as a function of day of year. The positive values of momentum flux are an extension of the synoptic scale pattern.

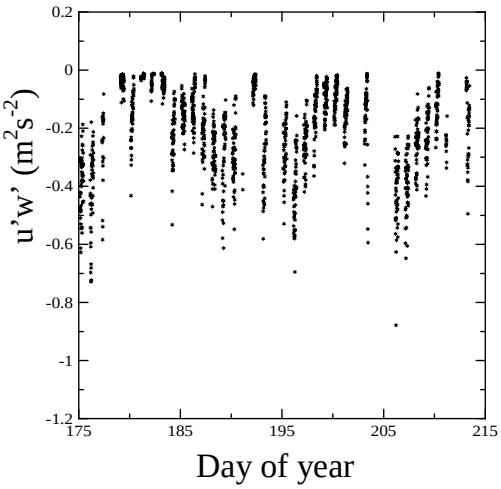

Figure 5 Calculated values of night time $\overline{u'w'}$ as a function of day of year. Although there is the same synoptic scale pattern, there are no significantly positive momentum fluxes.

In addition, all the TKE components follow a similar synoptic pattern, when $\overline{u'w'}$ values are

near zero, so are $\overline{u'u'}$, $\overline{v'v'}$, and $\overline{w'w'}$. The Reynolds stress correlation, R, is the momentum flux scaled by the standard deviations of u and w. The synoptic pattern is gone from the night time values (figure 7), but a small amount still exists for the day time R values (Figure 6). Flat plat boundary layer laboratory flows report –R values of 0.45 to 0.50. Reattached boundary layers yield smaller values of –R (Panigrahi and Acharya 2005). Canopy studies report –R values of about 0.4 at the canopy top and smaller values well below the canopy (Finnigan 2000).

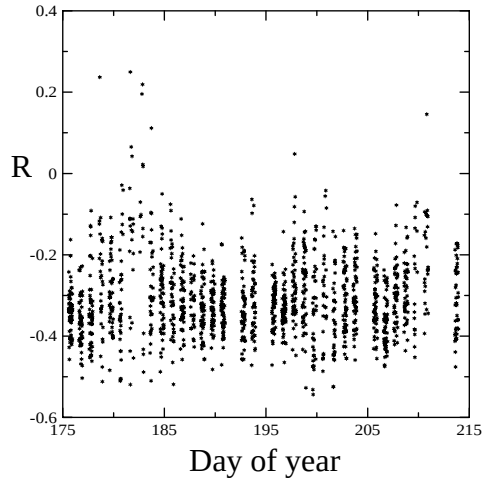

Figure 6 Calculated values of the day time correlation coefficient, R, as a function of day of year. Some synoptic scale pattern is still discernable.

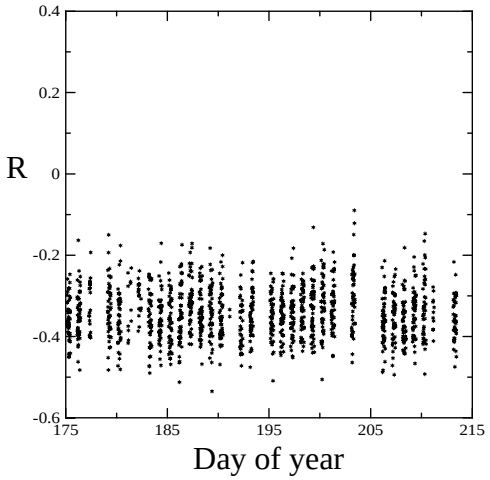

Figure 7 Calculated values of the night time correlation coefficient, R, as a function of day of year. No synoptic scale pattern is discernable.

5. MECHANISM

It is not clear from the data what mechanism might give rise to large quadrant 1 and quadrant 3 contributions to the momentum flux. It is possible that more than one mechanism is involved. We propose just one possible mechanism here.

Horizontal convergence of the wind direction near the surface (figure 8) can lead to not just an acceleration of the surface winds but also a net uplifting if the magnitude of the convergence near the surface is large enough. Both u' and w' will be greater than zero in this case creating a large scale quadrant 1 event. A horizontal divergence in the wind field will have the effect of reducing the local wind speed and also encourage a downdraft to fill in the diverging mass with fluid from above. This results in both u' and w' being negative and creates a large scale quadrant 3 event. The large peaks in the time series in figure 3 are consistent with this interpretation, but do not rule out other possible mechanisms.

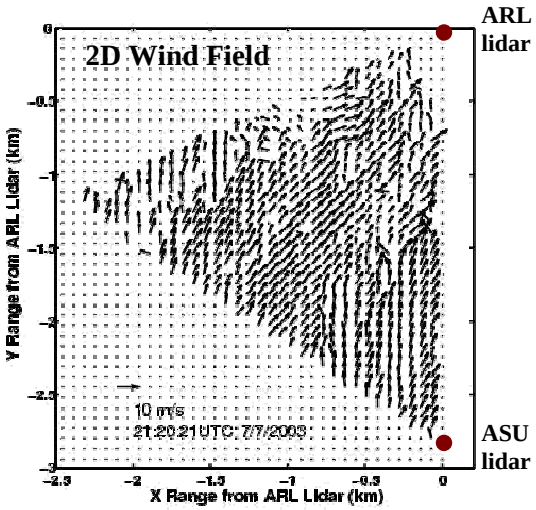

Figure 8 Wind speed and direction in a horizontal plane, z = 40-50m, just south of Oklahoma City, 2120 UTC, 7 July, 2003.

The wind field plot in figure 8 shows conditions during a typical day showing some regions of wind direction convergence and divergence. Unfortunately, there are no dual Doppler lidar scans for times when quadrant 1 and 3 events are dominant to compare to this typical day to verify that convergences were either more numerous or stronger or both.

6. IMPLICATIONS FOR CALCULATIONS

The presence of anomalously large quadrant 1 and 3 events, even if the total momentum transport is still downward, can lead to a measured value of $\overline{u'w'}$ that is significantly lower than expected given the amount of turbulence present at that time (figure 9).

No matter what the mechanism for the dominant quadrant 1 and 3 events, two large questions need to be addressed.

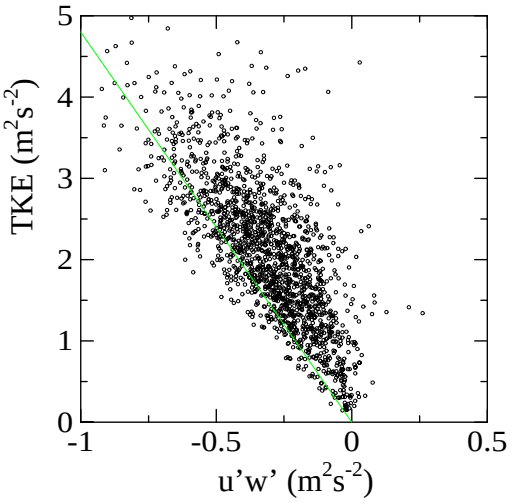

Figure 9 Turbulent kinetic energy as a function of momentum flux for all daytime data (1400-2259 UTC).

6.1. Similarity

Do these events violate the assumptions of similarity theories? Large horizontal convergences and divergences in the wind field lead to normally insignificant terms in the turbulence equations becoming significant. Notably, terms involving $\partial/\partial x$ and $\partial/\partial y$ may make significant contributions to the turbulence budgets. These terms are currently not measured by the usual point sensor arrays and may need to be known on too small a spatial scale for current remote sensing techniques.

6.2. Transport

Are these events significant transporters of pollutants? Although these events occur relatively rarely, they may still be a source of significant transport when they do occur. Further study is needed.

Acknowledgements

We thank the Joint Urban 2003 organizers and participants, with special thanks to the ARL instrument team for the tower set-up and data collection. Special thanks also to the attendees of the 9th George Mason University Transport and Diffusion conference for their input.

REFERENCES

Finnigan, J. J., 2000: Turbulence in plant canopies. *Annu. Rev. Fluid Mech*., **32**, 519-571.

Panigrahi, P. K. and S. Acharya, 2005: Excited turbulent flow behind a square rib. *Journal of Fluids and Structures*, **20**, 235-253.

Raupach, M. R., 1981: Conditional statistics of Reynolds stress in rough-wall and smooth-wall turbulent boundary layers. *J. Fluid Mech.*, **108**, 363-382.

Robinson, S. K., 1991: Coherent motions in the turbulent boundary layer. *Annu. Rev. Fluid Mech*., **23**, 601-639.

Wilczak, J. M., S. P. Oncley and S. A. Stage, 2001: Sonic anemometer tilt correction algorithms. *Bound.-Layer Meteor*., **99**, 127-150.